



AECL-11346

**Laser Plasma Generation of Hydrogen-free Diamond-like Carbon Thin Films on Zr-2.5Nb CANDU Pressure Tube Materials and Silicon Wafers with a Pulsed High-Power CO<sub>2</sub> Laser**

**Production par plasma laser de fines pellicules de carbone-diamant exempt d'hydrogène sur le Zr-2,5 Nb des tubes de force CANDU et les pastilles de silicium avec un laser au CO<sub>2</sub> pulsé à grande puissance**

N.A. Ebrahim, J.F. Mouris, C.R.J. Hoffmann, R.W. Davis, D.A. Guzonas

AECL

**Laser Plasma Generation of Hydrogen-free Diamond-like Carbon Thin  
Films on Zr-2.5Nb CANDU Pressure Tube Materials and Silicon  
Wafers with a Pulsed High-Power CO<sub>2</sub> Laser**

N.A. Ebrahim, J.F. Mouris, C.R.J. Hoffmann, R.W. Davis and D.A. Guzonas\*  
*\*Reactor Chemistry Branch*

Accelerator Physics Branch  
Chalk River Laboratories  
Chalk River, Ontario K0J 1J0  
1995 April

**AECL-11346**

EACL

**Production par plasma laser de fines pellicules de carbone-diamant exempt d'hydrogène sur le Zr-2,5 Nb des tubes de force CANDU et les pastilles de silicium avec un laser au CO<sub>2</sub> pulsé à grande puissance**

N.A. Ebrahim, J.F. Mouris, C.R.J. Hoffmann, R.W. Davis et D.A. Guzonas\*

\*Chimie des réacteurs

**RÉSUMÉ**

Nous donnons un compte rendu des premières expériences du dépôt par plasma laser de pellicules de carbone-diamant exempt d'hydrogène sur le Zr-2,5 Nb des tubes de force CANDU Zr-2,5 Nb et les substrats de silicium, en utilisant le laser au CO<sub>2</sub> à grande puissance et à impulsion courte du Laboratoire du laser à grande puissance des Laboratoires de Chalk River. Les pellicules ont été caractérisées en utilisant la spectroscopie Raman, les essais de microdureté Vickers et la microscopie à forces atomiques. Les minces pellicules présentent la signature caractéristique des pellicules carbone-diamant des spectres Raman obtenus en utilisant la laser à krypton ionisé (Kr<sup>+</sup>). Les essais de microdureté à très faible charge Vickers montrent la dureté de la surface enrobée d'environ 7 000 kgf/mm<sup>2</sup>, qui correspond à la dureté liée aux pellicules carbone-diamant. L'examen de microscopie à forces atomiques de la morphologie de la pellicule révèle que les cristaux de diamant sont répartis dans la pellicule, celle-ci ayant une épaisseur allant jusqu'à 0,5 µm produite par 50 impulsions laser. Avec bien plus d'impulsions laser, on pourrait s'attendre à obtenir des pellicules de carbone-diamant très uniformes. Ces expériences impliquent qu'il serait possible de déposer des pellicules carbone-diamant exempt d'hydrogène intéressantes pour les composants des réacteurs nucléaires avec un laser à haute puissance et à haute fréquence de répétition d'impulsions.

Physique des accélérateurs  
Laboratoires de Chalk River  
Chalk River (Ontario) K0J 1J0  
Juin 1995

AECL-11346

AECL

**Laser Plasma Generation of Hydrogen-free Diamond-like Carbon Thin  
Films on Zr-2.5Nb CANDU Pressure Tube Materials and Silicon  
Wafers with a Pulsed High-Power CO<sub>2</sub> Laser**

N.A. Ebrahim, J.F. Mouris, C.R.J. Hoffmann, R.W. Davis and D.A. Guzonas\*  
*\*Reactor Chemistry Branch*

**ABSTRACT**

We report the first experiments on the laser plasma deposition of hydrogen-free, diamond-like carbon (DLC) films on Zr-2.5Nb CANDU pressure-tube materials and silicon substrates, using the short-pulse, high-power, CO<sub>2</sub> laser in the High-Power Laser Laboratory at Chalk River Laboratories. The films were characterized using Raman spectroscopy, Vickers microhardness testing, and atomic force microscopy (AFM). The thin films show the characteristic signature of DLC films in the Raman spectra obtained using a krypton-ion (Kr<sup>+</sup>) laser. The Vickers ultra-low-load microhardness tests show hardness of the coated surface of approximately 7000 kg force mm<sup>-2</sup>, which is consistent with the hardness associated with DLC films. AFM examination of the film morphology shows diamond-like crystals distributed throughout the film, with film thicknesses of up to 0.5 μm generated with 50 laser pulses. With significantly more laser pulses, it is expected that very uniform diamond-like films would be produced. These experiments suggest that it should be possible to deposit hydrogen-free, diamond-like films of relevance to nuclear reactor components with a high-power and high-repetition-rate laser facility.

Accelerator Physics Branch  
Chalk River Laboratories  
Chalk River, Ontario K0J 1J0  
1995 June

**AECL-11346**

## I. INTRODUCTION

Recently there has been a great deal of interest in amorphous carbon thin films with diamond-like properties.<sup>1</sup> A material is amorphous if it has no detectable long-range order. Amorphous material with diamond-like characteristics results from random alternations between cubic and hexagonal geometries of carbon atoms. Although graphite, soot and carbon black all have the same chemical composition as diamond (i.e., all are forms of carbon), X-ray diffraction shows that they have very different crystal structures. Graphite consists of layers of condensed, six-membered two-dimensional aromatic rings of  $sp^2$ -hybridized carbon atoms (Fig. 1). It absorbs visible light and appears greyish-black. In the plane parallel to the aromatic network, graphite is a good electrical conductor. The lengths of the aromatic bonds in the ring system are 1.415 Å. The spacing between the layers, however, is 3.354 Å, because these atoms are held together by weaker van der Waals bonds. The layers can slide over each other, which makes graphite a soft material, suitable as a lubricant. Soot and carbon black are microcrystalline forms of graphite. Diamond has a different, but related, structure. Its crystallographic network consists exclusively of covalently bonded, three-dimensional aliphatic  $sp^3$ - hybridized carbon atoms arranged tetrahedrally, with a uniform distance of 1.545 Å between atoms (Fig. 2). The tetrahedrons connect to one another at their tips to form the crystal lattice. It is this structure of diamond that accounts for many of its extreme properties of hardness, resistance to wear, low-friction coefficient, electrical insulation, chemical resistance and optical transparency in the infrared. Single-crystal, impurity-free diamond is transparent in wavelength from the extreme ultraviolet through the visible spectrum to the near infrared (220 to 2500 nm) and from mid-infrared and beyond (wavelengths greater than 6000 nm).

Amorphous or partly-crystalline carbon films also display the properties of diamond, such as extreme hardness, high electrical resistivity, optical transparency in the infrared, and chemical resistance (Table I).<sup>1</sup> These macroscopic properties have been explained on the assumption that three-dimensional  $sp^3$  diamond-like bonds exist in the carbon films. Amorphous carbons are not only characterized by the deviation of atoms from their regular crystal lattice, but by different degrees of hybridization. Hence, atoms with tetrahedral  $sp^3$  (diamond-like) bonding as well as trigonal  $sp^2$  (graphite-like) bonding should exist in amorphous carbon. The high hardness of, and the strong bonding to, substrates make these films particularly attractive as a means of improving the fretting-wear resistance of Zr-2.5Nb CANDU\* pressure tubes, and perhaps improving the lifetime of critical components in CANDU reactor fueling machines.

In this report we describe the first experiments on the laser plasma generation of hydrogen-free, diamond-like carbon (DLC) films on Zr-2.5Nb CANDU pressure-tube materials using the short-pulse, high-power,  $CO_2$  laser in the High-Power Laser Laboratory at Chalk River Laboratories. DLC films have also been deposited on Si (110) substrates. The films were characterized using Raman spectroscopy, Vickers microhardness testing, and atomic force microscopy (AFM).

## II. EXPERIMENTAL CONSIDERATIONS

A schematic of the experimental arrangement is shown in Figs. 3 and 4. The short-pulse  $CO_2$  laser facility has been discussed in detail elsewhere,<sup>2,3,4</sup> and only the essential points are restated. For these experiments, the facility was configured for a single wavelength operation to produce up to 55 J at 10.59  $\mu m$ . The laser pulsewidth was approximately 500 ps full-width at half-maximum (FWHM), with a linear risetime of approximately 200 ps. The 10-cm diameter laser beam was focused with an off-axis, diamond-turned parabolic mirror to a nearly-diffraction-limited spot. With an f-number of 12.5, the focusing mirror

---

\* CANDU: CANada Deuterium Uranium; registered trademark.

was designed to produce a focal spot of diameter approximately 250  $\mu\text{m}$  and a focal depth of approximately 15 mm (Fig. 3). The focal power density of the beam was then expected to approach  $2 \times 10^{14}$   $\text{W}/\text{cm}^2$ .

The graphite target was approximately 1.5 cm square, and mounted inside the vacuum chamber so that the laser beam made an angle of approximately  $20^\circ$  with the normal to the graphite surface (Fig. 4). The graphite was heated under vacuum to  $200^\circ\text{C}$  for 24 hours, to drive off as much moisture as possible. The graphite target was moved after each laser shot, so that ablation occurred from a new surface. The substrate to be coated consisted of a specimen of Zr-2.5Nb, approximately 1.5 cm square, that had been electropolished and annealed. It was mounted approximately 5 cm from the graphite, with its surface parallel to the graphite surface. The vacuum in the chamber was approximately  $5 \times 10^{-6}$  torr. Substrates of Si  $\langle 110 \rangle$  wafers were also coated with DLC films.

### III. EXPERIMENTAL RESULTS

Substrates exposed to the ion fluxes from the hot plasma near the graphite surface were coated with a thin film. A transparent deposit layer was visible to the naked eye after less than five laser pulses. At focal power densities of  $2 \times 10^{14}$   $\text{W}/\text{cm}^2$ , it was expected that the plasma generated on the surface of the graphite feedstock would be hot enough ( $\sim 250$  eV at a density of  $\sim 10^{20}$   $\text{cm}^{-3}$ ) to produce fully stripped carbon ions (C<sup>VI</sup>), which would stream across the gap to the Zr-2.5Nb specimen. The resulting coating was expected to contain atoms with tetrahedral  $sp^3$  (diamond-like) bonding. Similar coatings were applied to Si  $\langle 110 \rangle$  substrates. The existence of diamond-like films on Zr-2.5Nb and Si $\langle 110 \rangle$  was established by observing the characteristic features of the diamond-like structures in the Raman spectra from such films, measurements of Vickers microhardness, and AFM.

#### (i) Raman Spectroscopy

Raman spectra are sensitive to changes in translational symmetry, and hence are useful for the study of disorder and crystallite formation in carbon films. The excitation of the Raman spectra were performed with a krypton-ion ( $\text{Kr}^+$ ) laser operating at a wavelength of 647.1 nm at a power level of 50 mW, and detected using a 1.0 m single monochromator equipped with a liquid-nitrogen-cooled CCD (charge-coupled device) detector. A holographic notch filter was used for additional stray light rejection. Band frequencies were calibrated against a mercury calibration lamp and are accurate to  $\pm 1$   $\text{cm}^{-1}$ . However, the error in the band positions of the broad features in the DLC film spectra may be greater, because of difficulties in defining the exact band centre.

The first-order Raman spectrum of highly-ordered, pyrolytic graphite shown in Fig. 5a consists of a single sharp peak at  $1581$   $\text{cm}^{-1}$ . A second Raman band has been reported<sup>5</sup> at  $42$   $\text{cm}^{-1}$ , but was outside the range of the Raman system used in this work. The first-order Raman spectrum for industrial diamond (Fig. 5b) consists of a single sharp peak at  $1333$   $\text{cm}^{-1}$ . A weak, broad feature to higher frequency is probably from imperfections or impurities in the industrial diamond sample. For the POCO graphite used in these experiments, the first-order Raman spectrum (Fig. 6b) consists of a peak at  $1583$   $\text{cm}^{-1}$ , which results from the in-plane vibrations of the layers (see Fig. 1), and a second broad peak at  $1334$   $\text{cm}^{-1}$ , which is ascribed to structural imperfections associated with in-plane vibrations. Under laser irradiation these peaks are significantly broadened (Fig. 6a), with peak intensities occurring at  $1583$   $\text{cm}^{-1}$  and  $1335$   $\text{cm}^{-1}$ .

Figure 7a shows a first-order Raman spectrum of a Si $\langle 110 \rangle$  substrate with the normal silicon peak at  $520$   $\text{cm}^{-1}$ . A second, weak peak is observed at approximately  $950$   $\text{cm}^{-1}$  (Fig. 7a and 7b), possibly from a surface film of silicon oxide. Fig. 8a and 8b show a first-order Raman spectrum of a laser-generated thin

film deposited on this Si(110) substrate. This film was deposited with 100 laser pulses, each containing between 4 and 5 joules of energy, with the resulting focused power density of approximately  $2 \times 10^{13}$  W/cm<sup>2</sup>. In addition to the silicon peaks at 520 cm<sup>-1</sup> and 950 cm<sup>-1</sup>, the Raman spectrum now also shows a broad triangular structure peaking at approximately 1560 cm<sup>-1</sup>, with a base stretching from 1000 cm<sup>-1</sup> to 1700 cm<sup>-1</sup>. This feature is generally considered to be a signature of DLC in the film<sup>6</sup>. We can fit this Raman profile to a peak at 1408 cm<sup>-1</sup> and a peak at 1520 cm<sup>-1</sup>, as shown in Fig. 8c.

Figure 9 shows a series of first-order Raman spectra of a thin, laser-generated film on a specimen of Zr-2.5Nb CANDU pressure-tube material taken from different locations on the specimen. The different locations (spot 1 through 6) on the specimen are indicated in Fig. 10. The film was deposited with 50 laser pulses of approximately 50 joules per pulse, with a focused power density of  $2 \times 10^{14}$  W/cm<sup>2</sup>. The Zr-2.5Nb sample was not rotated between the laser pulses, and so the film deposition may be somewhat irregular across the specimen. The Raman spectra at all six locations on the specimen show the characteristic signature of the DLC film, with the broad triangular structure peaking at ~1350 and ~1560 cm<sup>-1</sup>, with a base stretching from 1000 to 1600 cm<sup>-1</sup>. The intensity of the Raman scattering and the frequencies of the two maxima were found to vary significantly with location on the surface. A decrease in the frequency of the low-frequency peak was associated with an increase in the frequency of the high-frequency peak. Table II summarises the locations of the various peaks and the relative intensities of the Raman spectra at various locations on the specimen. The Raman spectrum at location 5 is replotted on an expanded vertical scale in Fig. 11. A distinct peak at approximately 1335 cm<sup>-1</sup> is apparent (c.f. spectrum of diamond in Fig. 5b).

#### (ii) Vickers Microhardness

The Vickers microhardness values, HV (in units of kg force mm<sup>-2</sup>), were measured<sup>7</sup> at a number of points on the film using a hardness tester capable of applying a loading force of 0.005 N in a controlled manner. Vickers hardness of the diamond-like films was compared to the values obtained from the Zr-2.5Nb substrate on the uncoated side. A significant increase in the hardness of the coated surface was evident. Hardness measurements of diamond-like films give microhardness values HV  $\approx$  7000 kg force mm<sup>-2</sup>. For comparison, hardness measurements of the uncoated Zr-2.5Nb substrate give microhardness values HV  $\approx$  700 kg force mm<sup>-2</sup>.

#### (iii) Atomic Force Microscopy

A Nanoscope II AFM was used to image the diamond-like films deposited on the Zr-2.5Nb substrate. The surface was cleaned with methanol and blown dry under a high-pressure nitrogen stream before imaging, to remove surface contamination and dust. Images were acquired at 15 spots on the surface. The Section routine in the Nanoscope II software, which provides height and distance information along user-defined slices across an AFM image, was used to measure the dimensions of features in the image, and to estimate the film thickness.

Fig. 12a shows an 18  $\mu$ m  $\times$  18  $\mu$ m topview AFM image acquired in the darker-colored region of the sample. In this image, the height information is encoded in the gray scale, with black being the lowest (0 nm) and white being the highest (1000 nm). The surface consists of large, relatively smooth (on this scale) areas interspersed with regions containing large, sharp crystals that range from 100 to 400 nm in diameter. Fig. 12b shows a 5  $\mu$ m  $\times$  5  $\mu$ m three-dimensional view illustrating one of the crystalline regions.

The difference in height between the highest and lowest areas in Fig. 12a is 400 nm, indicating that the film thickness in this region is at least 400 nm. An examination of the data from all 15 spots indicates that the film thickness varies from < 40 nm in the light-colored areas to 500 nm in the dark-colored areas. This is consistent with the Raman data, which gave higher intensity in the darker regions. It was noted that the amount of the surface covered by the large, sharp crystals was greater just outside the darker-colored region of the sample than within that region. In the very light-colored regions of the sample, the film was thin enough that polishing scratches and the grain structure of the underlying substrate could be distinguished.

At higher magnification, the smooth areas in Fig. 12a consisted of small crystallites roughly 40 nm in diameter. This small structure was found at every one of the 15 spots examined. Figs. 13 and 14 show 5000 nm × 5000 nm three-dimensional views of two areas on the sample that show different crystalline regions. Fig. 15 shows a 500 nm × 500 nm three-dimensional view of a region on the sample that shows very large crystals. The largest crystal in this image is 400 nm × 200 nm.

#### IV. CONCLUSIONS

We have conducted the first experiments on the laser plasma deposition of hydrogen-free, DLC films on Zr-2.5Nb CANDU pressure-tube materials as well as silicon substrates, using the short-pulse, high-power, CO<sub>2</sub> laser in the High-Power Laser Laboratory at Chalk River Laboratories. The thin films show the characteristic signature of diamond-like carbon films in the Raman spectra obtained using a krypton-ion (Kr<sup>+</sup>) laser. The Vickers ultra-low-load microhardness tests show hardness of the coated surface of approximately 7000 kg force mm<sup>-2</sup>, which is consistent with the hardness associated with DLC films. Film thicknesses of up to 0.5 μm have been obtained with 50 laser pulses. With significantly more laser pulses, it is expected that uniform diamond-like films would be produced. These experiments suggest that it should be possible to deposit hydrogen-free, diamond-like films of relevance to nuclear reactor components with a high-power and high-repetition-rate laser facility.

#### V. ACKNOWLEDGEMENTS

The authors thank R.J. Kelly, R. Backwell and J.F. Weaver for technical support, D. Proulx for engineering design support, J. Ungrin for support and encouragement during the course of this work and F. Amouzouvi for hardness measurements and useful discussions.

#### V. REFERENCES

1. C.B. Collins, F. Davanloo, T.J. Lee, J.H. You and H. Park, *American Ceramic Society Bulletin*, **71**, No. 10, 1535 (1992).
2. N.A. Ebrahim, *Physics in Canada*, **46**, No. 6, 178 (1989).
3. N.A. Ebrahim, *Research Trends in Physics*, Ed. A.M. Prokhorov, AIP (1992), pp. 310 - 351.
4. N.A. Ebrahim, J.F. Mouris and R.W. Davis, Atomic Energy of Canada Limited Report, AECL-11240 (1994).
5. S.A. Solin, *Physica*, **99B**, 443 (1980).
6. S.S. Wagal, E.M. Juengeman and C.B. Collins, *Appl. Phys. Lett.* **53** (3), 187 (1988).
7. We thank L. Clegg and F. Amouzouvi of Whiteshell Laboratories for the hardness measurements.

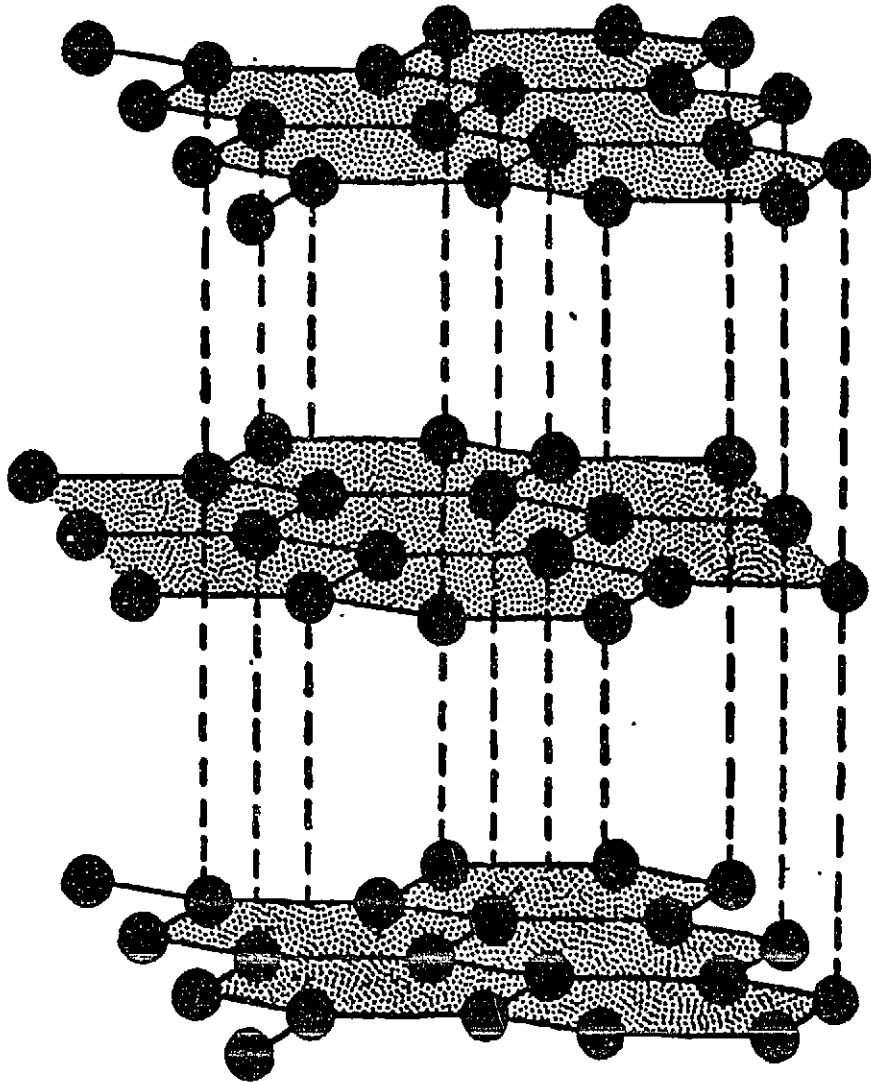
**Table 1. Comparison of Crystalline Diamond and Amorphic Diamond Film**

<b>Property</b>	<b>Crystalline Diamond</b>	<b>Amorphic Diamond</b>
<b>Fabrication Pressure</b>	7.7 GPa	$10^{-6}$ torr
<b>Fabrication Temperature</b>	2150° C	35° C
<b>Maximum Surface Area</b>	1 cm <sup>2</sup>	> 100 cm <sup>2</sup>
<b>Hardness</b>	90 GPa	35 - 40 GPa
<b>Young's Modulus</b>	1200 GPa	300 - 4 GPa
<b>Coefficient of Friction</b>	0.1	0.1 - 0.15

**Table II. Positions of Peaks in the Raman Spectra of Diamond-like Carbon Films**

Location (See Fig. 3)	Low-Frequency Peak ( $\text{cm}^{-1}$ )	High-Frequency Peak ( $\text{cm}^{-1}$ )	Peak Intensity (Arbitrary Units)
1	1357	1555	280
2	1341	1556	632
3	1351	1560	4580
4	1364	1537	1017
5	1335	1578	1481
6	1344	1560	250

Fig. 1. Crystal structure of graphite.



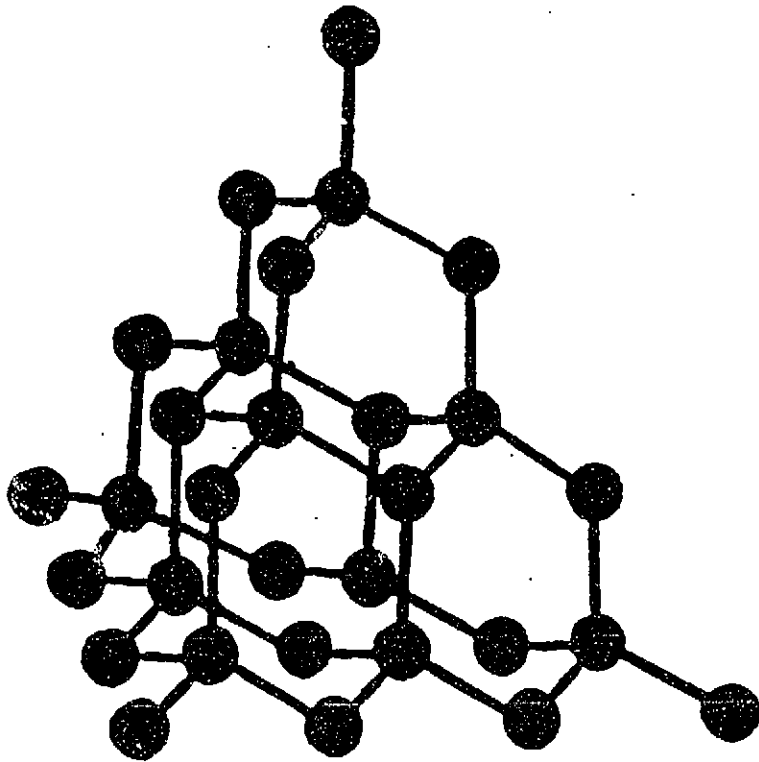


Fig. 2. Crystal structure of diamond.

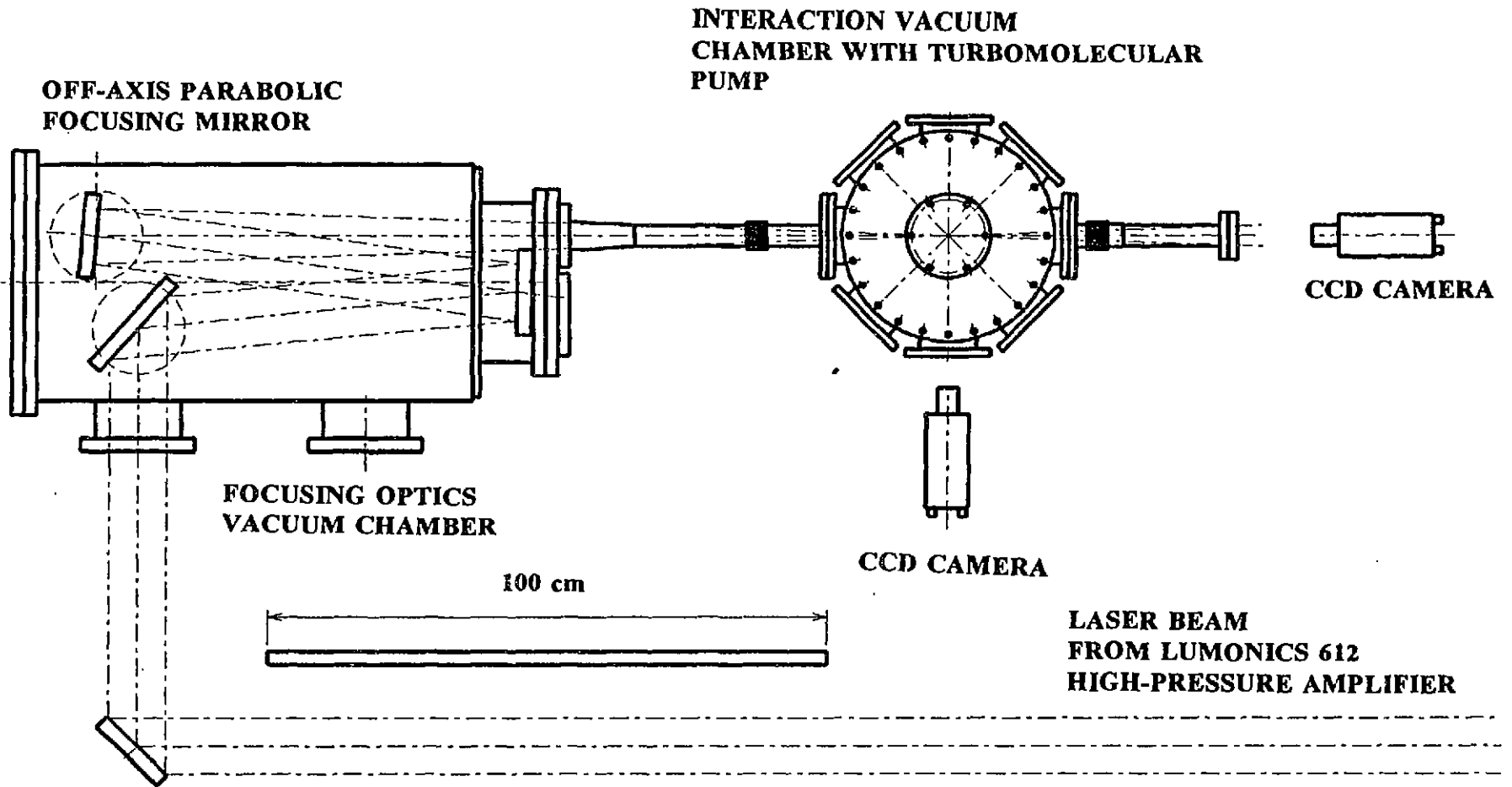
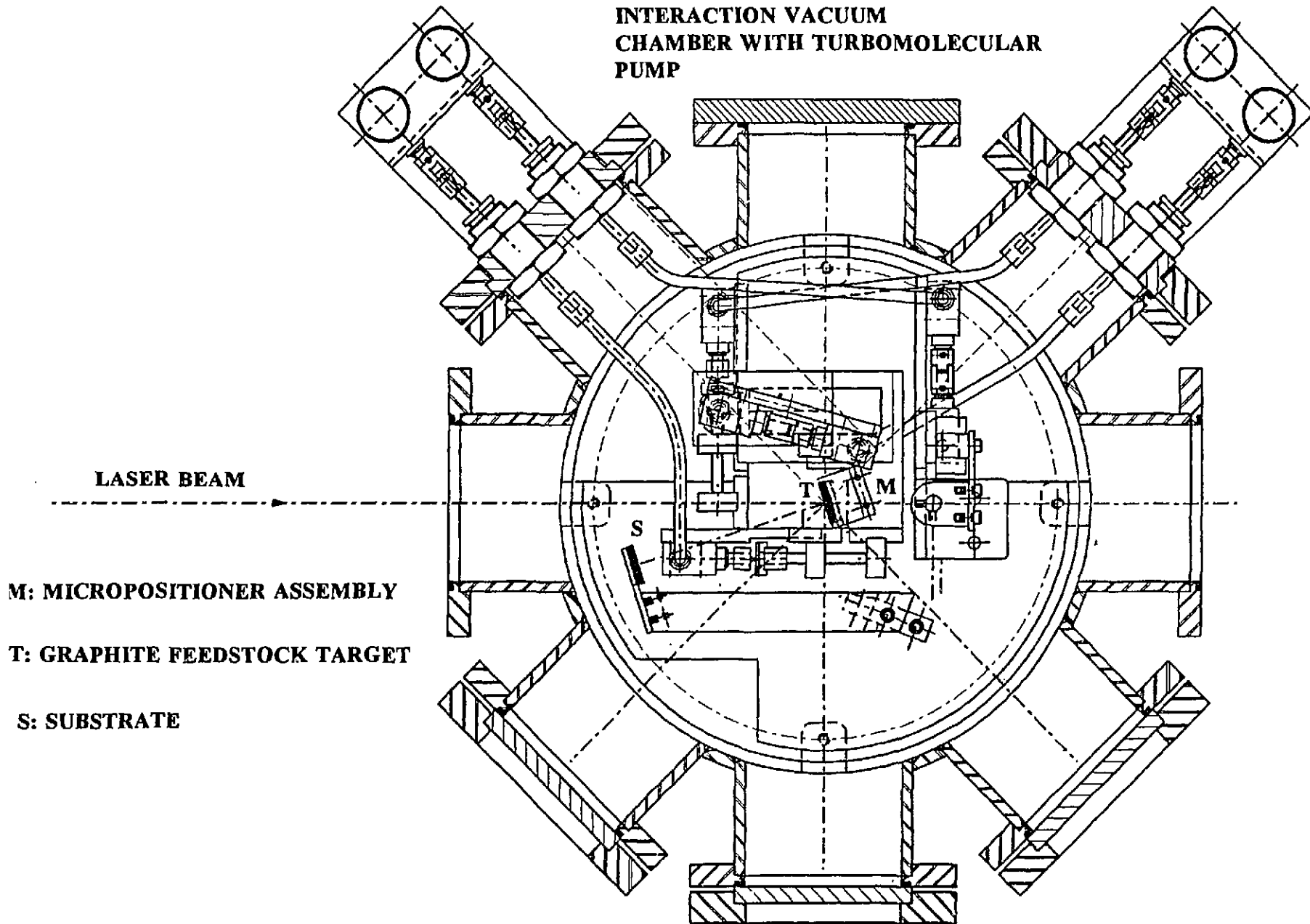


Fig. 3. Schematic of experimental arrangement.

**MICROPOSITIONER DRIVE**

**MICROPOSITIONER DRIVE**

**INTERACTION VACUUM  
CHAMBER WITH TURBOMOLECULAR  
PUMP**



**LASER BEAM**

**M: MICROPOSITIONER ASSEMBLY**

**T: GRAPHITE FEEDSTOCK TARGET**

**S: SUBSTRATE**

**Fig. 4. Schematic details of the vacuum chamber.**

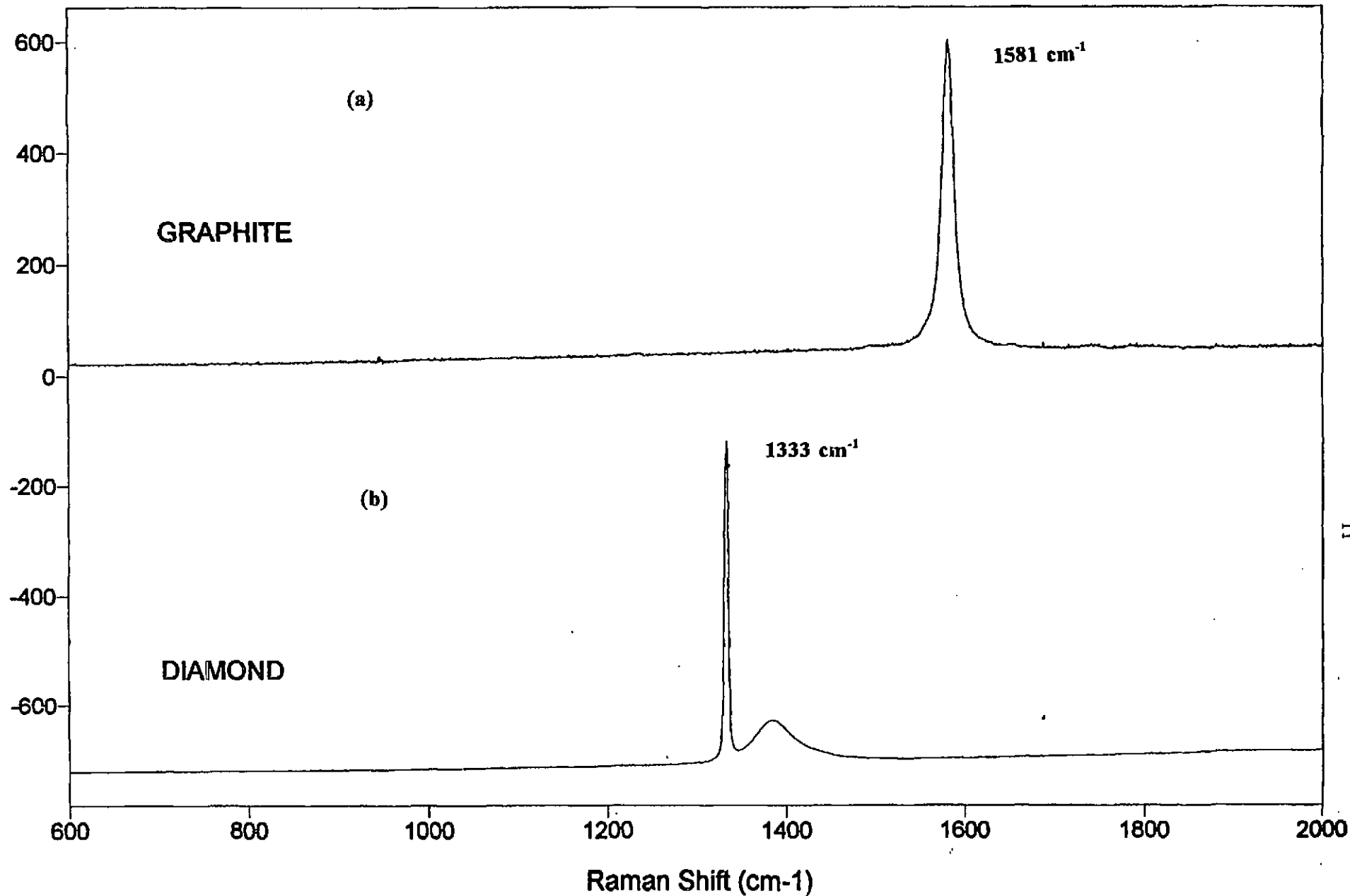


Fig. 5. (a) First-order Raman spectrum of highly-ordered pyrolytic graphite (HOPG). The peak is at 1581 cm<sup>-1</sup>. (b) First-order Raman spectrum of industrial diamond. The peak is at 1333 cm<sup>-1</sup>. The feature at the longer wavenumbers is probably from impurities.

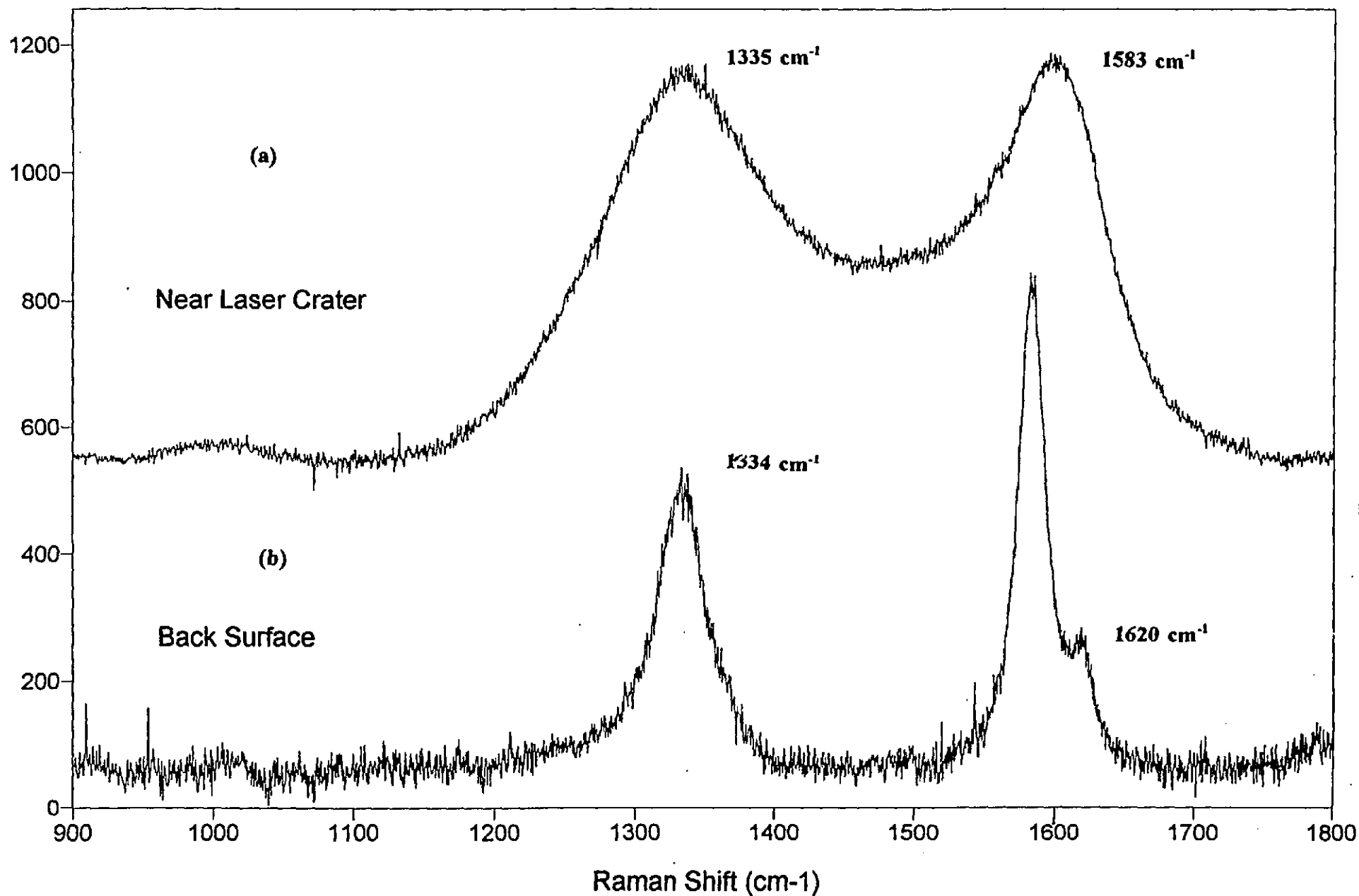


Fig. 6. (a) First-order Raman spectrum of POCO graphite on the back surface (unirradiated surface). The peak at  $1583\text{ cm}^{-1}$  is due to the in-plane vibrations of the layers. The second peak at  $1335\text{ cm}^{-1}$  is ascribed to structural imperfections associated with in-plane vibrations. (b) First-order Raman spectrum of laser-irradiated POCO graphite near a laser crater. Note the broadening of the lines and a small frequency shift as well.

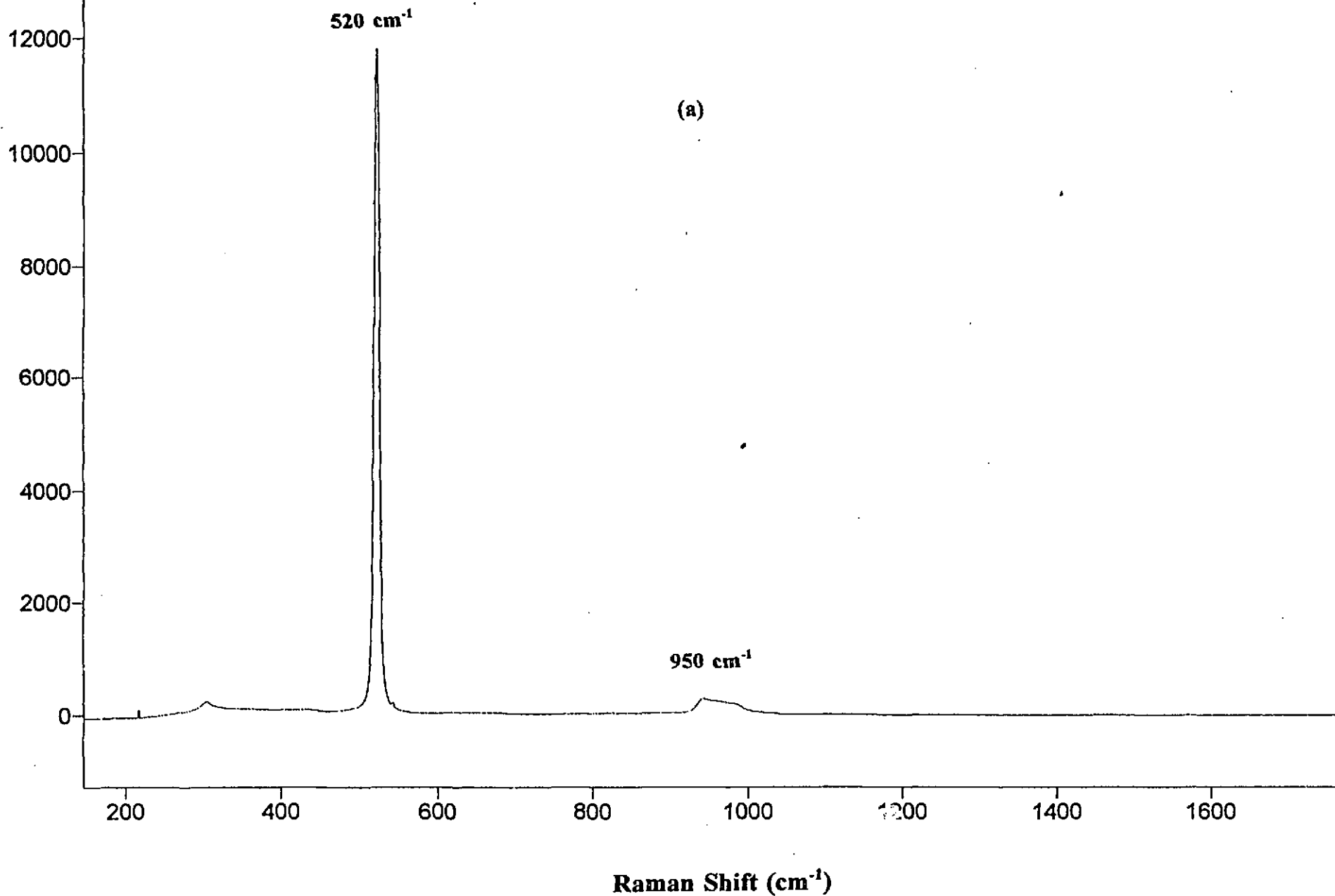
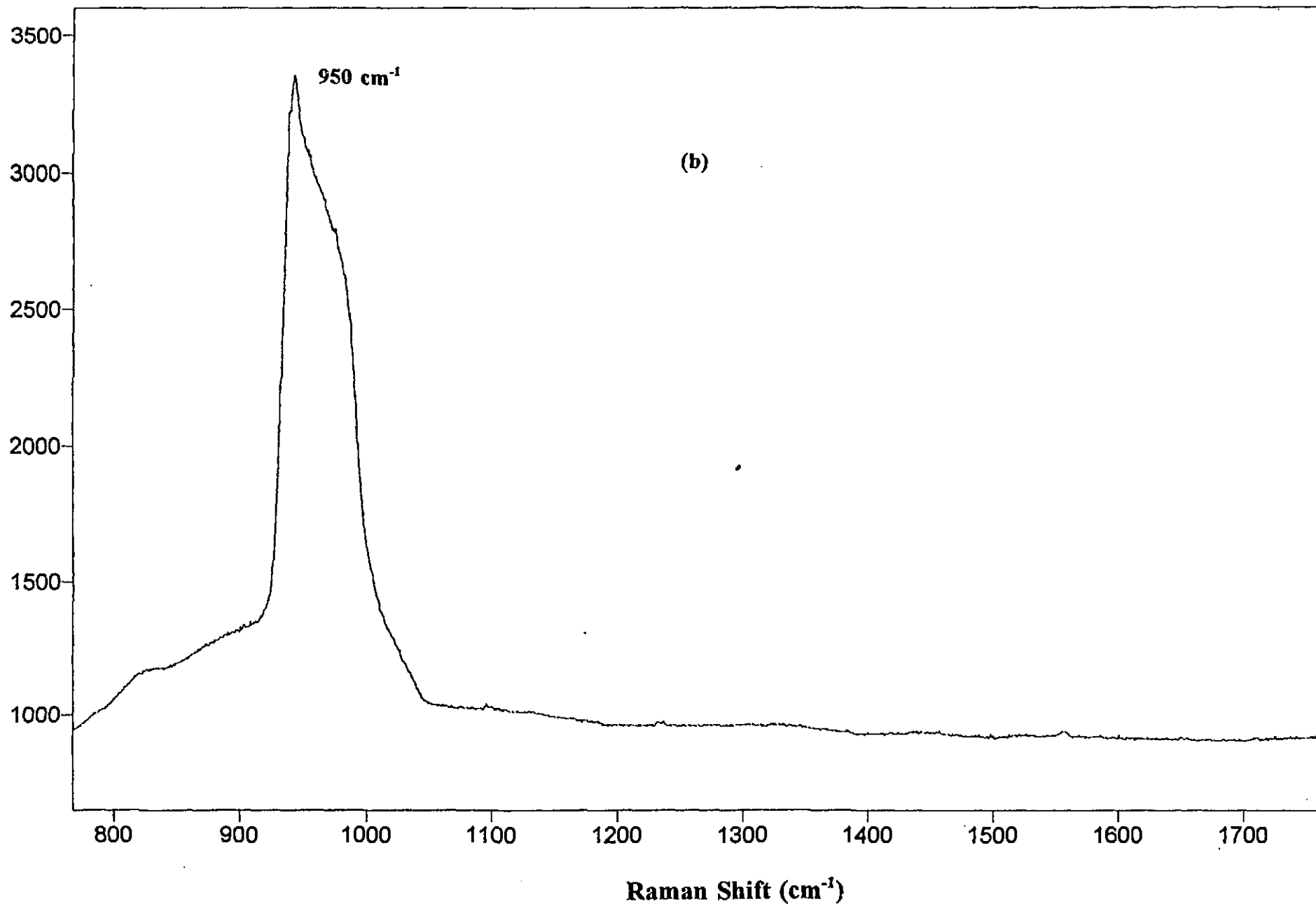


Fig. 7. (a) First-order Raman spectrum of Si(110) substrate with the silicon line at 520 cm<sup>-1</sup>. The smaller feature at 950 cm<sup>-1</sup> (expanded in Fig. 7b) is probably from silicon oxide on the surface.



**Fig. 7. (b)** The 800 -1800 cm<sup>-1</sup> region of the Raman spectrum of Si<110> from Fig. 7(a) is replotted with an expanded vertical scale. The feature at 950 cm<sup>-1</sup> is probably from silicon oxide. No features are seen in the spectrum above ~1050 cm<sup>-1</sup>.

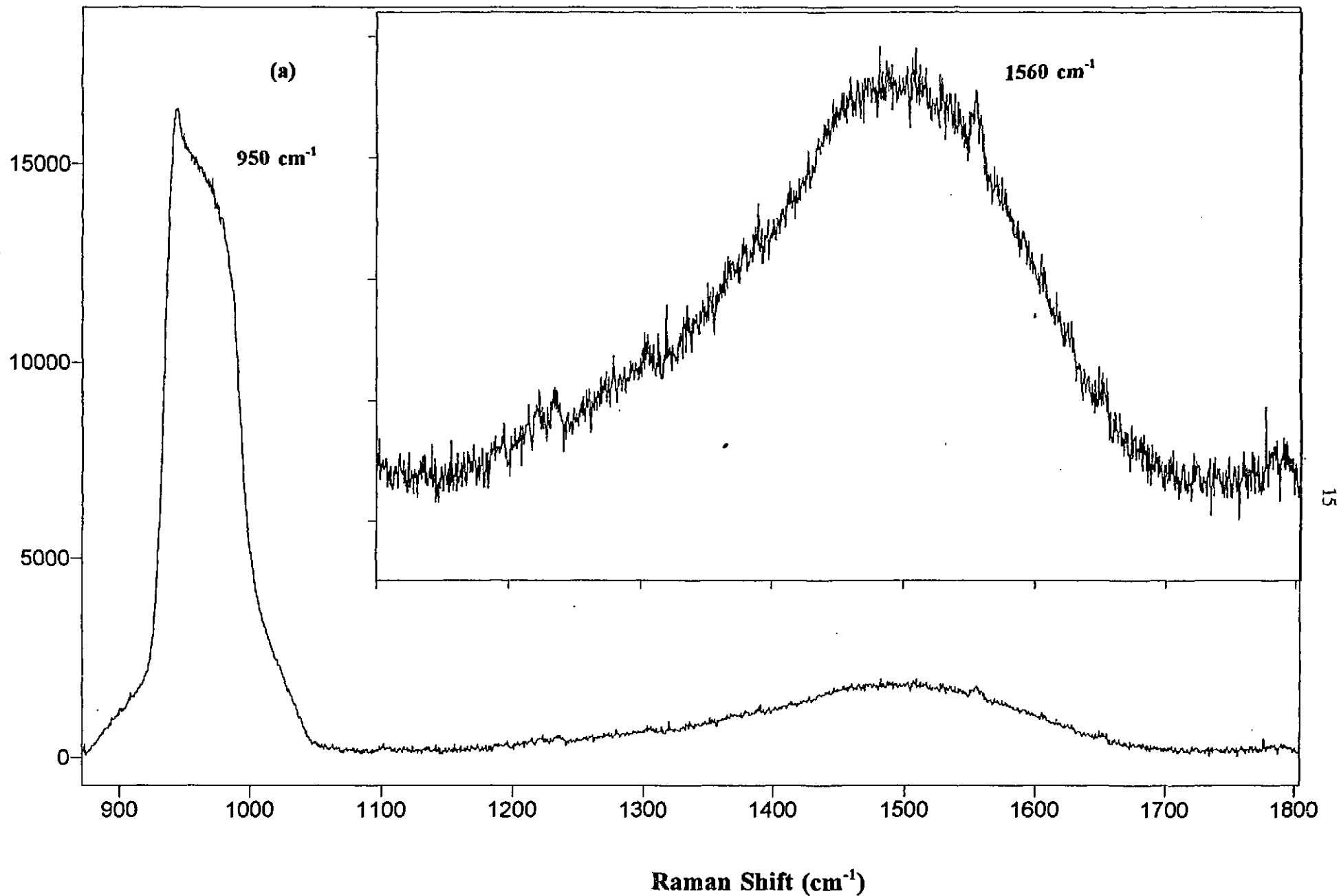


Fig. 8. (a) First-order Raman spectrum of a laser-generated thin film on Si  $\langle 110 \rangle$  substrate showing the broad triangular structure peaking at approximately  $1560\text{ cm}^{-1}$  with a base stretching from  $1000\text{ cm}^{-1}$  to  $1700\text{ cm}^{-1}$ , which is indicative of a diamond-like carbon film. The feature is expanded in the inset of this figure. The feature at  $950\text{ cm}^{-1}$  is probably from silicon oxide. The silicon line at  $520\text{ cm}^{-1}$  from the silicon substrate is shown in Fig. 8(b).

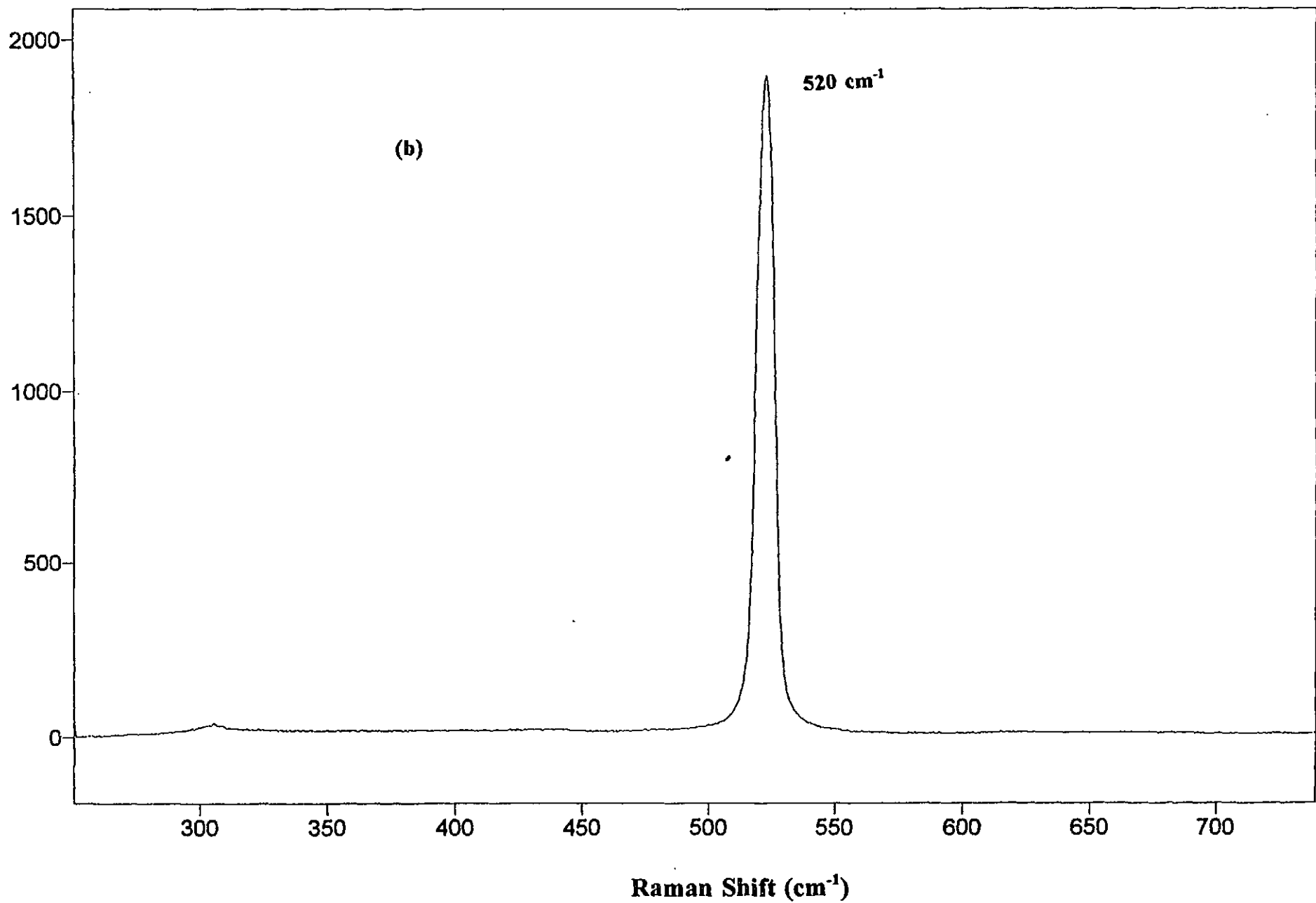


Fig. 8. (b) The silicon line at 520 cm<sup>-1</sup> from the silicon substrate.

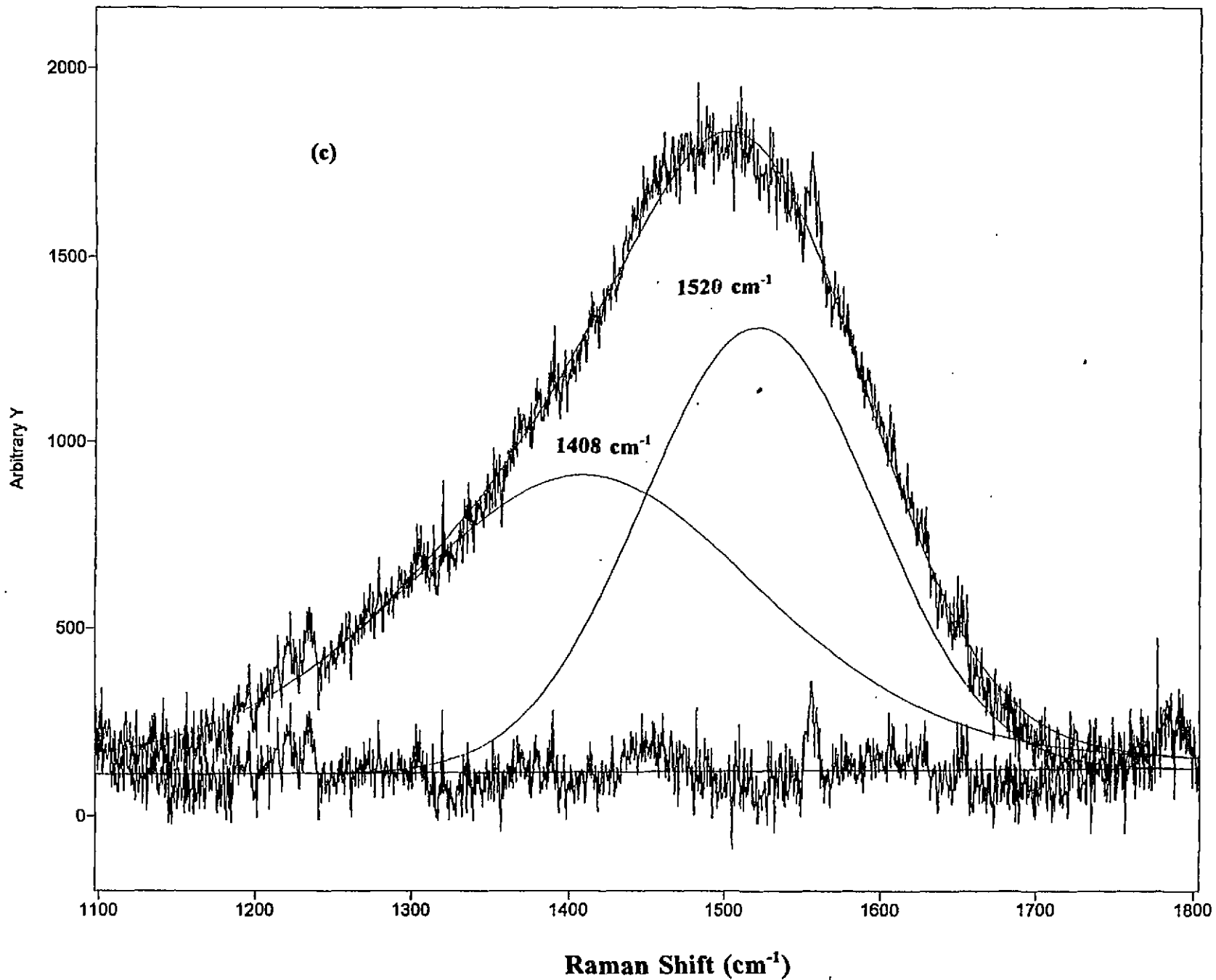


Fig. 8. (c) Line fit to the Raman profile from Fig. 8a, with two peaks at 1408  $\text{cm}^{-1}$  and 1520  $\text{cm}^{-1}$ .

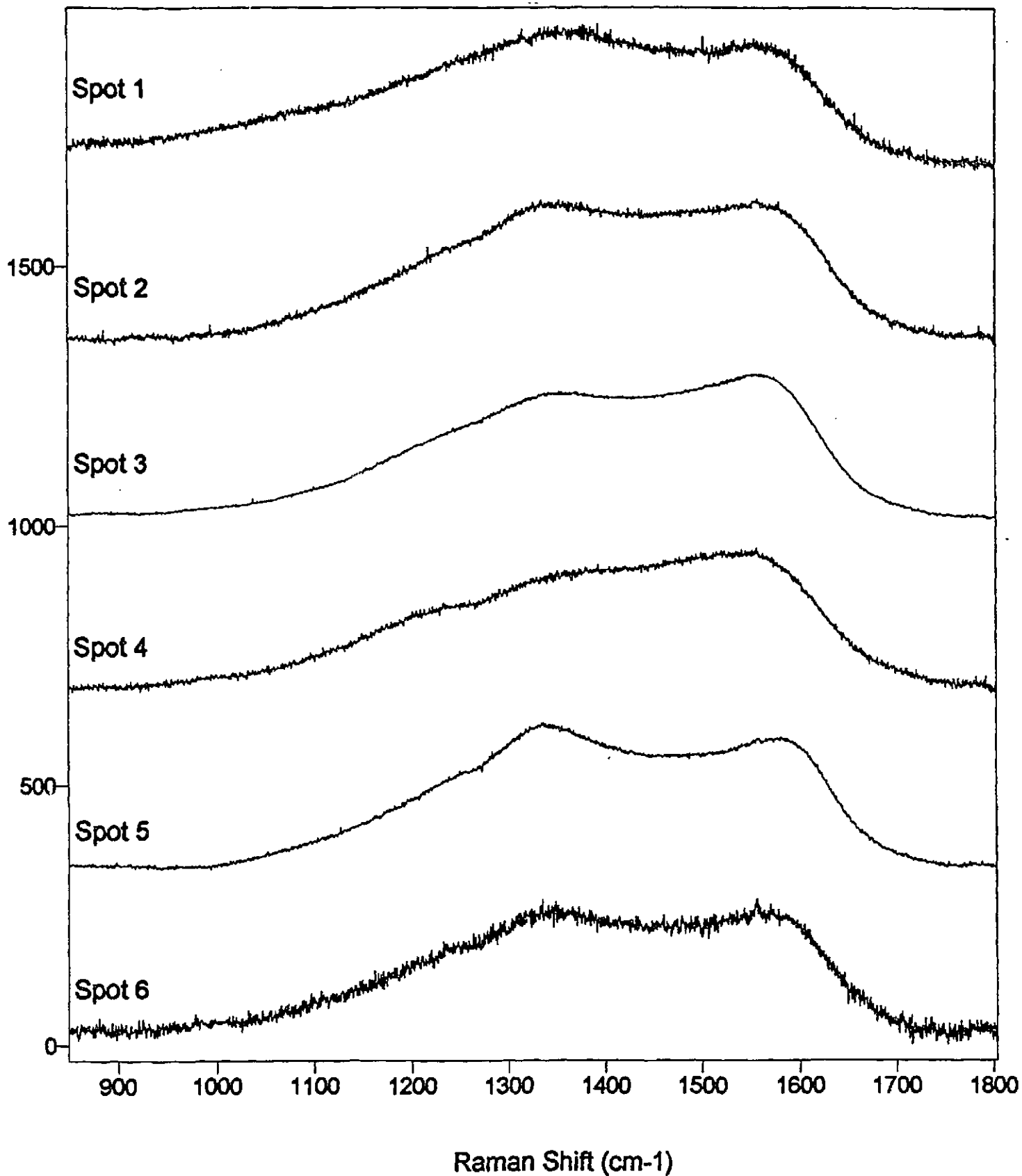
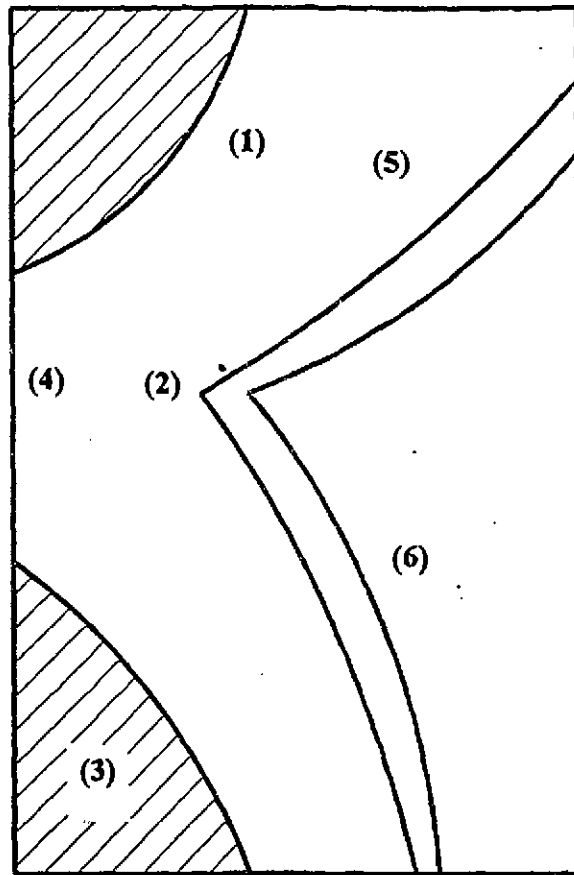
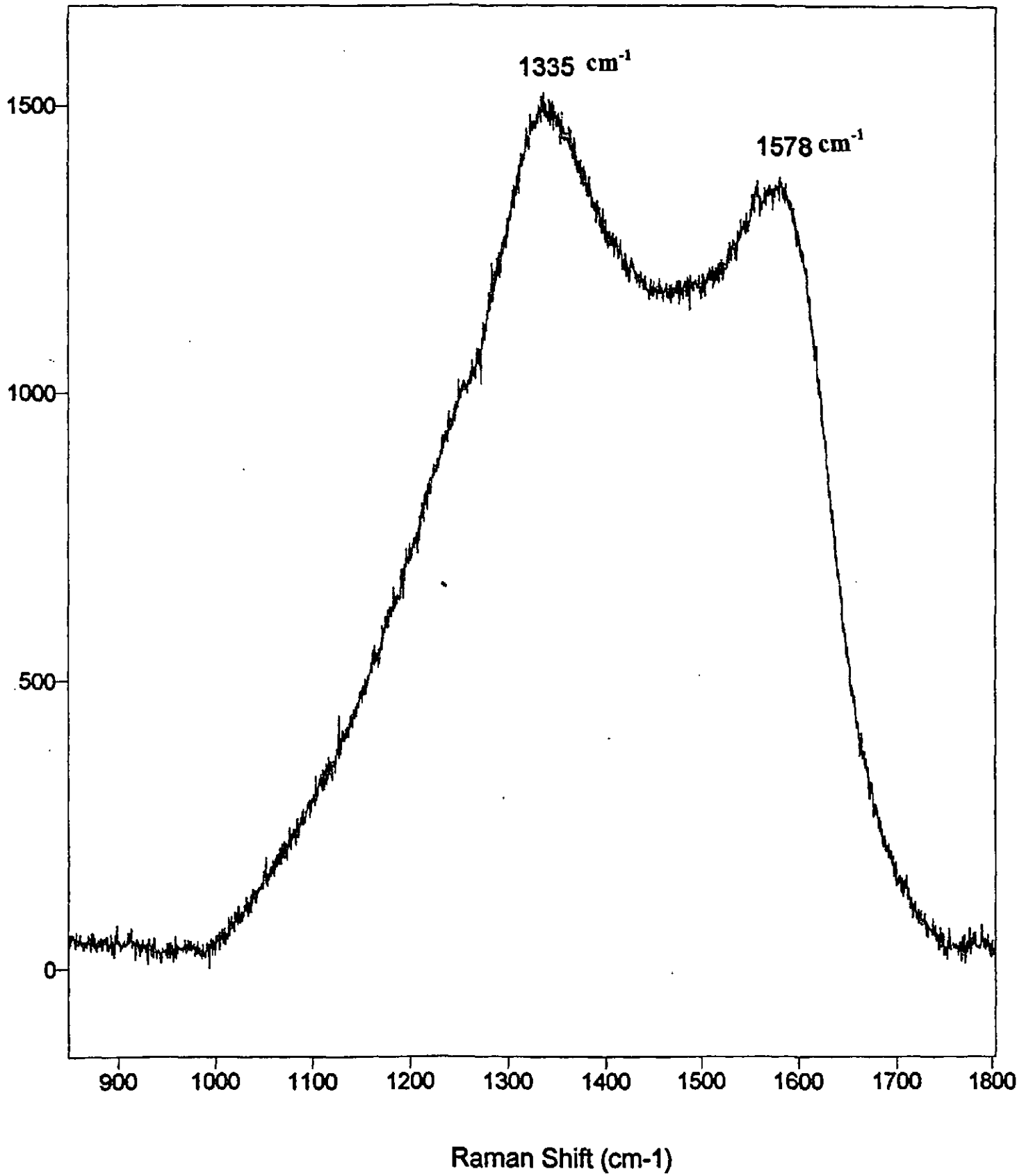


Fig. 9. First-order Raman spectra of laser-generated thin film on Zr-2.5Nb substrate at locations indicated on Fig. 10. Note the broad triangular structure peaking at  $1560\text{ cm}^{-1}$ , with a base stretching from  $1000$  to  $1600\text{ cm}^{-1}$ .



**Fig. 10.** Map of the locations on the Zr-2.5Nb specimen where the Raman spectra were obtained. The lines indicate approximate locations of distinct changes in the coloration of the surface film. The cross-hatched areas were much darker in color than the rest of the sample.



**Fig. 11.** The Raman spectrum at location 5 (in Fig. 10) on an expanded vertical scale. Note the peak at 1335 cm<sup>-1</sup>.

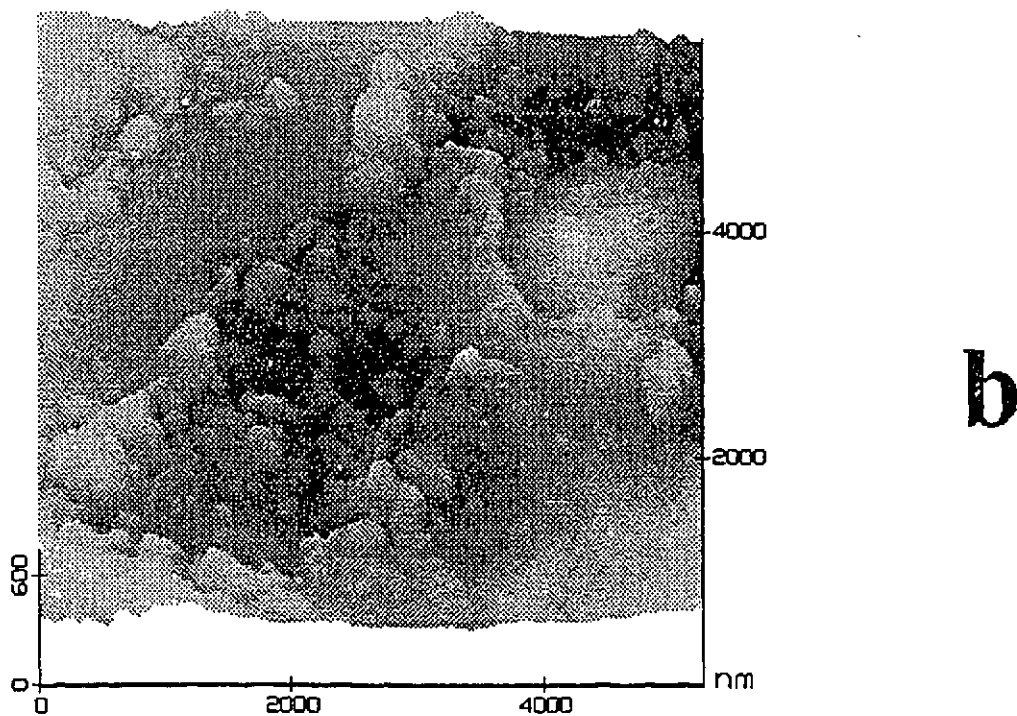
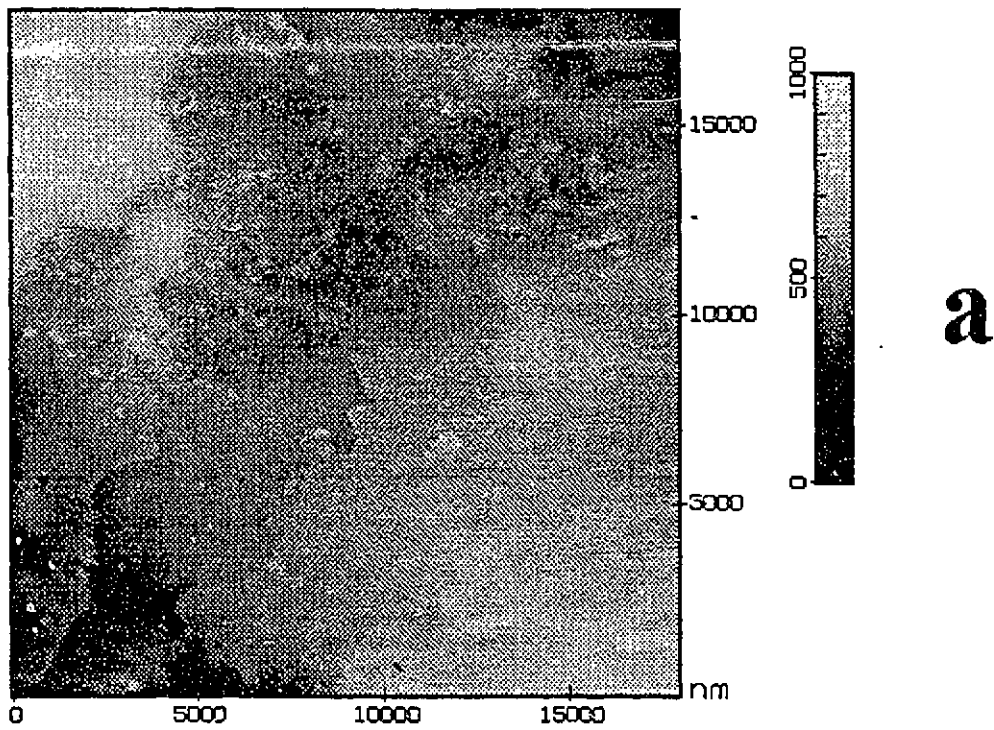


**Fig. 12.** (a) An  $18\ \mu\text{m} \times 18\ \mu\text{m}$  topview AFM image acquired in the darker-colored region of the sample. (b) A  $5000\ \text{nm} \times 5000\ \text{nm}$  three-dimensional view illustrating one of the crystalline regions.

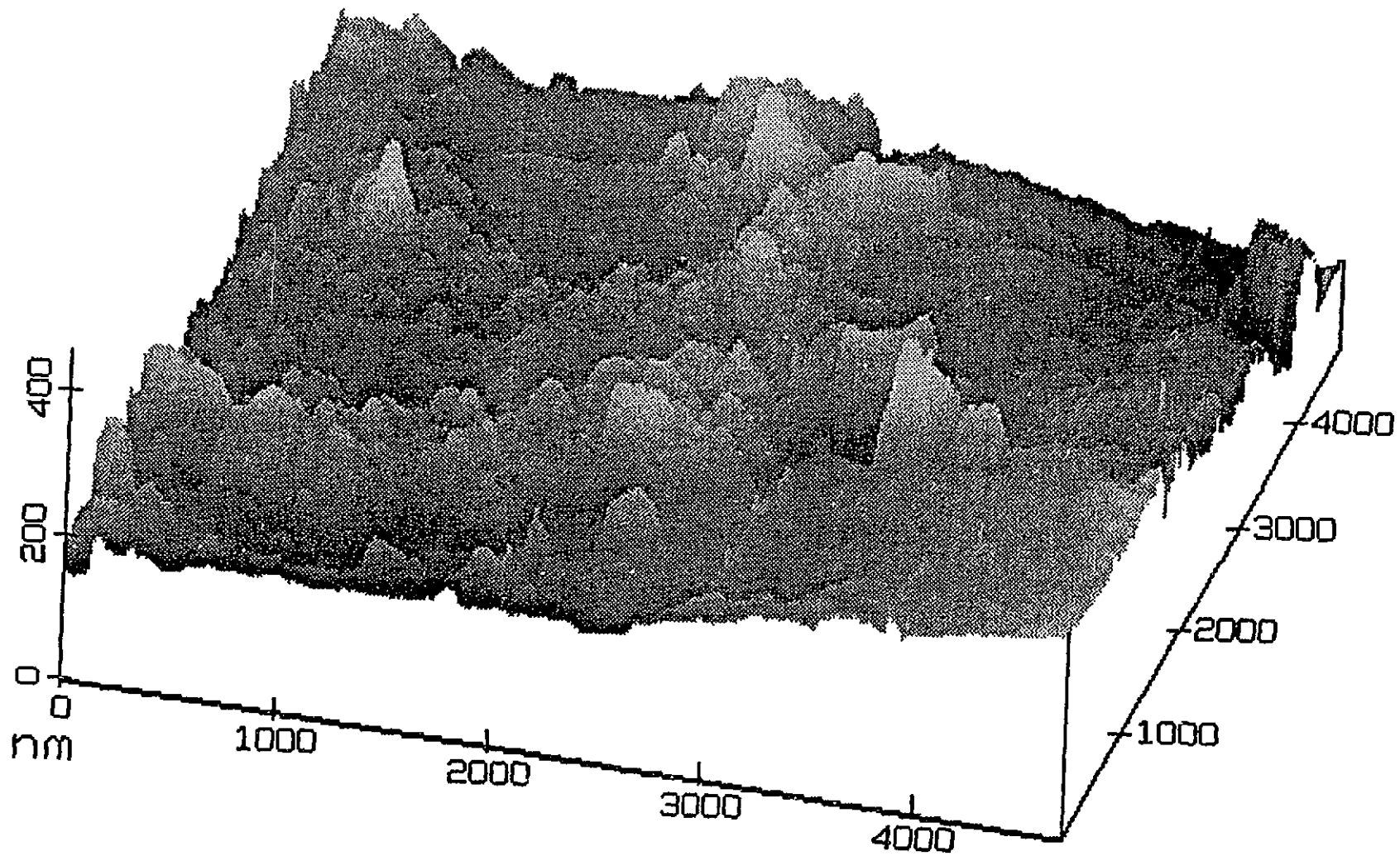


Fig. 13. A 5000 nm  $\times$  5000 nm three-dimensional view illustrating one of the crystalline regions.

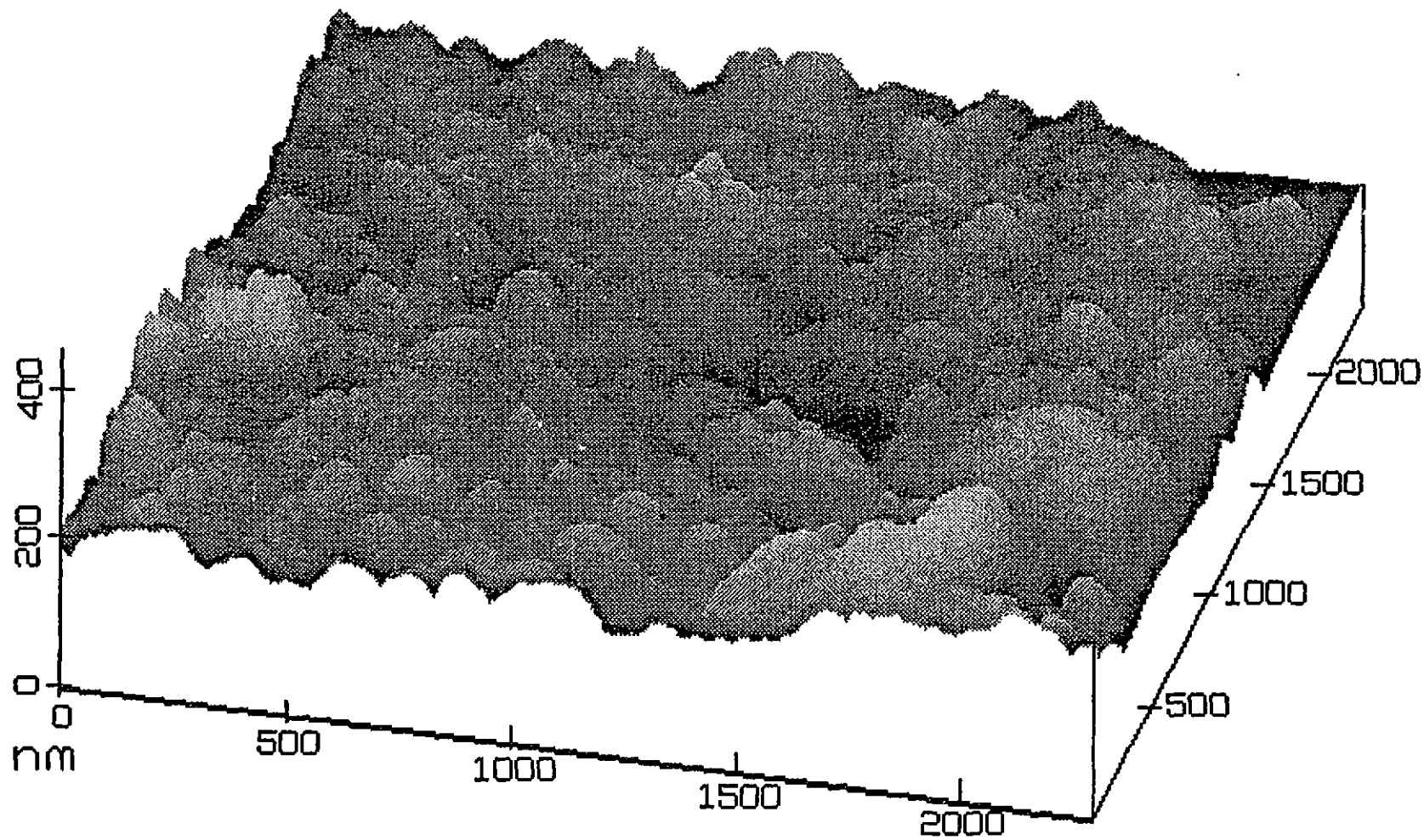
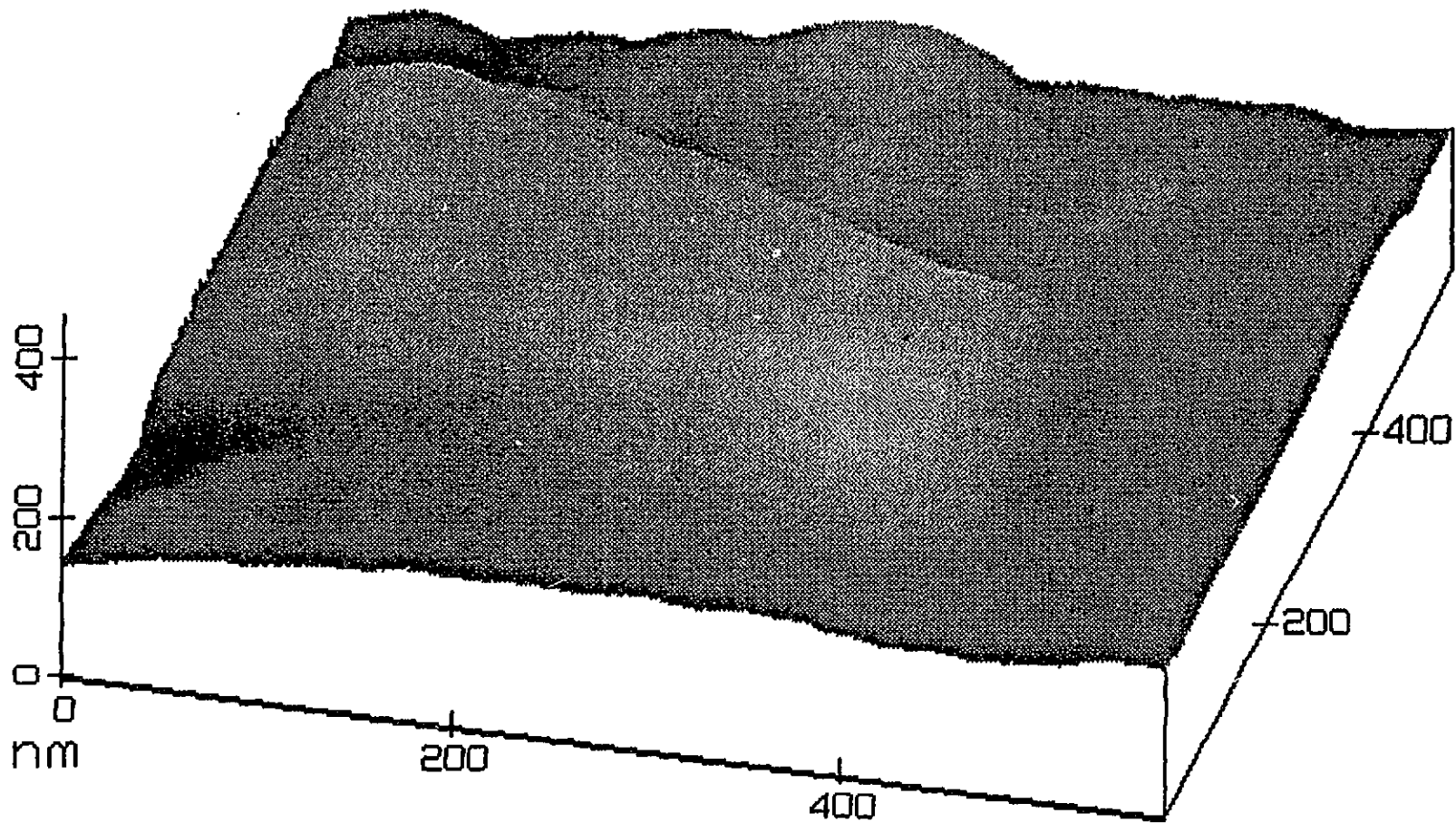


Fig. 14. A 5000 nm × 5000 nm three-dimensional view illustrating one of the crystalline regions.



**Fig. 15.** A 500 nm  $\times$  500 nm three-dimensional view illustrating one of the crystalline regions with very large crystals.

Cat. No. /No de cat.: CC2-11346E

ISBN 0-660-16207-5

ISSN 0067-0367

To identify individual documents in the series, we have assigned an AECL- number to each.

Please refer to the AECL- number when requesting additional copies of this document from:

Scientific Document Distribution Office (SDDO)

AECL

Chalk River, Ontario

Canada K0J 1J0

Fax: (613) 584-1745

Tel.: (613) 584-3311

ext. 4623

Price: A

Pour identifier les rapports individuels faisant partie de cette série, nous avons affecté un numéro AECL- à chacun d'eux.

Veuillez indiquer le numéro AECL- lorsque vous demandez d'autres exemplaires de ce rapport au:

Service de Distribution des Documents Officiels

EACL

Chalk River (Ontario)

Canada K0J 1J0

Fax: (613) 584-1745

Tél.: (613) 584-3311

poste 4623

Prix: A

